

AUG 12 1963

UNCLASSIFIED

AERE - R 4347



MASTER

United Kingdom Atomic Energy Authority  
RESEARCH GROUP  
Report

THE EMISSION  
OF XENON-133 FROM LIGHTLY IRRADIATED  
URANIUM DIOXIDE SPHEROIDS AND POWDERS

D. DAVIES G. LONG

Chemistry Division,  
Atomic Energy Research Establishment,  
Harwell, Berkshire.

1963

© - UNITED KINGDOM ATOMIC ENERGY AUTHORITY - 1963

Enquiries about copyright and reproduction should be addressed to the  
Scientific Administration Office, Atomic Energy Research Establishment,  
Harwell, Didcot, Berkshire, England.

U.D.C.

661.879.12-179: 546.295.02.133

546.295.02.133

## **DISCLAIMER**

**Portions of this document may be illegible in electronic image products. Images are produced from the best available original document.**

THE EMISSION OF XENON-133 FROM LIGHTLY  
IRRADIATED URANIUM DIOXIDE SPHEROIDS AND POWDERS

by

D. Davies and G. Long

ABSTRACT

The post-irradiation heating technique has been applied to determine the emission of Xenon-133 from uranium dioxide in the form of both spheroids and powders. For sintered spheroids and powders the xenon emission data are consistent with those obtained previously for sintered compacts, ( $E = 70$  kcal/mole,  $D_{1400} = 5 \times 10^{-15}$  cm<sup>2</sup>/sec). No variations in diffusion coefficient due to differences in mode of preparation or in the degree of sub-division of the uranium dioxide were detected. Plasma-fused spheroids, on the other hand, after annealing to remove imperfections show a high value for the activation energy (100 kcal/mole) and a lower value of diffusion coefficient at 1400°C ( $4 \times 10^{-16}$  cm<sup>2</sup>/sec).

Chemistry Division,  
U.K.A.E.A. Research Group,  
Atomic Energy Research Establishment,  
HARWELL

June, 1963

HL63/3101 (C.4)

PD

B/F

## CONTENTS

	<u>Page</u>
INTRODUCTION	1
EXPERIMENTAL	1
RESULTS AND DISCUSSION	2
ACKNOWLEDGEMENTS	4
REFERENCES	4

## TABLES

I	Physical Properties of $\text{UO}_2$ Spheroids and Powders	5
II	Diffusion Parameters of $\text{UO}_2$ Spheroids and Powders	6

## ILLUSTRATIONS

<u>fig.</u>	
1	Plots of $\log_{10}(D/a^2)$ versus $1/T^{\circ}\text{K}$ for sintered spheroids of Group A.
2	Plots of $\log_{10}(D/a^2)$ versus $1/T^{\circ}\text{K}$ for sintered spheroids of Group B.
3	Plot of $\log_{10}(D/a^2)$ versus $1/T^{\circ}\text{K}$ for plasma fused spheroids, as-received.
4	Plot of $\log_{10}(D/a^2)$ versus $1/T^{\circ}\text{K}$ for plasma fused spheroids, annealed in vacuum at $1650^{\circ}\text{C}$ .
5	Plot of $\log_{10}(D/a^2)$ versus $1/T^{\circ}\text{K}$ for samples of $\text{UO}_2$ powder.
6	Plot of $\log_{10}D$ versus $1/T^{\circ}\text{K}$ for the sintered spheroids and powders.

## INTRODUCTION

The post irradiation heating technique has been applied to study the emission of Xenon-133 and of volatile fission products from a variety of lightly irradiated samples of spheroidal and powdered uranium dioxide. The objectives of the investigation were two-fold: firstly to measure the quality of the spheroidised uranium dioxide with respect to gas release, and secondly to seek any differences that there may be in the diffusion parameters of massive uranium dioxide (sintered compacts) and these more finely divided specimens. In this respect the powder specimens are of interest since in the two reported instances of high values of the diffusion coefficient and low activation energy<sup>(1, 2)</sup> the data were obtained on finely divided materials.

## EXPERIMENTAL

### Heating Experiments

Full details of the equipment and experimental techniques are described elsewhere<sup>(3)</sup>. Briefly, approximately 1g of a sample of uranium dioxide containing natural uranium, or the equivalent weight of enriched sample, was reduced in carbon monoxide at 800°C. It was then enclosed in a small aluminium capsule, sealed under vacuum in a silica ampoule and irradiated in a flux of  $1.2 \times 10^{12}$  n.cm<sup>-2</sup>sec<sup>-1</sup> for a period of 2 days, (total dose  $2.4 \times 10^{17}$  nvt). After cooling for about 7 days to allow short-lived fission gas activity and iodine-133 precursor to decay the sample was transferred to a molybdenum crucible in a tungsten-wound furnace and heated at a series of increasing temperatures in the range 800 to 1600°C for periods of about 2 hours. During the heating any evolved xenon-133 was swept in a stream of hydrogen to a flow counter. The counting rate and total counts recorded by this counter are proportional to the emission rate and total evolution respectively. In order to determine the total xenon content of the sample it was dissolved in 75% nitric acid and the evolved xenon again swept through the flow counter.

The results were analysed in terms of the equivalent sphere model by plotting the fraction (f) released as a function of the square root of the heating time (t). The simplified form of the diffusion equations appropriate to the experimental conditions<sup>(1)</sup> is

$$f = \frac{6}{\pi} \frac{1}{2} \left( \frac{D}{a^2} t \right)^{\frac{1}{2}}$$

where D is the diffusion coefficient and a the equivalent sphere radius.

The slope of the plot is therefore a measure of the diffusion time-constant,  $D/a^2$ , which is commonly indicated by  $D'$ . From  $D'$  the diffusion coefficient itself is determined by eliminating the equivalent sphere radius. This is obtained from a B.E.T. determination of the free surface area (S cm<sup>2</sup>/g) of the sample<sup>(4)</sup>:-

$$a = 3/\rho S \text{ cm}$$

where  $\rho$  is the sample density (g/cm<sup>3</sup>).

In common with the sintered specimens investigated previously<sup>(6)</sup>, all the samples examined in this study showed an initial high release of activity - an initial burst - whenever the temperature of the sample was raised. The experimental observations were analysed in such a way as to minimise the importance of the burst<sup>(5)</sup> and its presence was subsequently ignored.

The diffusion studies reported have covered two preparations of powders, six sintered specimens of uranium dioxide spheroids and two samples of fused spheroids. The preparative techniques are described below, and the relevant physical properties summarised in Table I.

Powder Specimens were prepared by precipitation of ammonium diuranate from nitrate solution and calcination at 900°C in air, followed by reduction in hydrogen at the same temperature. The preparation was divided into two portions; both were annealed in hydrogen for 5 hrs., one at 1250°C and the other at 1650°C. The latter preparation sintered during annealing and was therefore crushed to pass 400 mesh. Finally both preparations were reduced in carbon monoxide at 800°C immediately prior to irradiation.

Sintered Spheroids, Group A. These were prepared by spheroidising fragments of green compacts of uranium dioxide in a gyratory mill. Densification was achieved by sintering in cracked ammonia at 1650°C. Finally the required size fractions were produced by sieving.

Sintered Spheroids, Group B. These were prepared by blending uranium dioxide powder with binder to produce a granular mix. After sieving out the appropriate size range the granules were densified by rotation in a gyratory mill and finally sintered.

Fused Spheroids were prepared by passing fragments of sintered compacts through the flame of a plasma torch. Any material which had by-passed the torch was separated by rolling the product down an inclined plane. A portion of each of the two preparations studied was annealed in vacuo for 2 hours at 1650°C and cooled slowly in order to relieve any stress.

## RESULTS AND DISCUSSION

The relationships between  $\log_{10} (D/a^2)$  and the reciprocal of the absolute temperature are plotted in Figures 1 to 5, and the relevant diffusion parameters are presented in Table II.

### Quality of the spheroids

Both intuitively and from previous work on sintered compacts <sup>(6)</sup> it is anticipated that good fission product retention demands, in the first instance, that the free surface area available for the escape of fission products should be as small as possible. For sintered compacts specimens have been produced with a B.E.T. surface area as low as a few  $\text{cm}^2/\text{g}$ ; on the other hand the lower limit attainable with spheroidised material is set by the geometric area. For spheroids of radius  $100\mu$  this amounts to about  $30 \text{ cm}^2/\text{g}$ , and any imperfections such as cracks or porosity may substantially increase this figure. A useful measure of the degree of perfection of a batch of spheroids is given by the roughness factor, the ratio of the observed to geometric surface area. This is only an approximate guide, since in estimating the geometric area it is usual to take the mean radius of the batch, while in fact a weighted mean area, taking into account particle size distribution, is required.

Roughness factors for the samples studied are quoted in Table I. In general the observed area approximates fairly closely to the geometric, the roughness factors lying in the range 1.2 to 1.6 for most of the sintered specimens and for the annealed fused material.

Exceptions are the "as-prepared" fused material and the sintered samples B1(b) and B3. The high values of the former are attributed to crazing of the surface resulting from the high rate of quenching from the plasma torch, the crazing being removed in the subsequent annealing. For the two sintered samples the high roughness factor is believed to be spurious. The B.E.T. measurement may be considerably in error since only a small weight of sample was available, and the equipment was working near its limit. This conclusion is supported by the low fission gas release results quoted below.

Several of the sintered specimens, notably A2 and B2, showed a large single crescent-shaped pore in their metallographic sections. It is assumed that this is in fact a section of a lenticular pore, but the micrograph does not show whether or not it is connected to the surface. A measurement of the open porosity of the sample will give some information, but neither metallographic examination nor open porosity measurements can give even an indication of the internal surface area of the sample. A large single pore open to the surface will contribute significantly to the open porosity but may contribute very little to the total surface area, while the converse is true for a network of fine pores, which may well be undetected on metallographic examination. For example, in a spheroid of radius  $150\mu$  an open disc-shaped pore of radius  $80\mu$  and mean width  $10\mu$  contributes only an additional 14% to the surface area [roughness factor = 1.14] but contributes 1.4% to the open porosity. On the other hand in the same spheroid a network of fine pores of diameter  $0.1\mu$ , and total open porosity of 0.1% produces a roughness factor of 2.5.

An independent measure of the quality of the spheroids is obtained by comparing the observed value of the diffusion time constant ( $D'$ ) at  $1400^{\circ}\text{C}$  with that calculated assuming that the diffusion constant of  $5 \times 10^{-15} \text{ cm}^2/\text{sec}$  obtained for compacts at  $1400^{\circ}\text{C}$  (6) applies and that the equivalent sphere radius can be taken to be equal to the mean geometric radius of the spheroids. In Table II the square root of the ratio of the observed and calculated values of  $D'$  is presented, since the calculated gas release in a fuel element is, for small release, proportional to  $\sqrt{D'}$  (6). As with the criterion of surface area, this measure of the spheroid quality also indicates that they are of good quality and that the method of preparation has no detectable effect on the degree of perfection of the spheroids.

#### Diffusion Data

Results for the individual samples studied are presented in Figures 1 to 5, and the parameters derived from these plots are collated in Table II.

It is of interest to compare the data of Table II with the diffusion parameters obtained by the same technique for sintered compacts (6) namely

$$D_{1400} = 5 \times 10^{-15} \text{ cm}^2/\text{sec}, \quad E = 70 \pm 5 \text{ kcal/mole}$$

In making the comparisons of the diffusion coefficients it should be borne in mind that probable errors are large, since the difference in coefficient for both the reference standard (compacts) and the samples to be compared are obtained by combining the square of the experimental observations, namely the slope of an  $f$  vs  $\sqrt{t}$  plot and a surface area determination. The latter in particular is probably subject to substantial variable errors. A value of  $D_{1400}$  for spheroids lying in the range 1 to  $10 \times 10^{-15} \text{ cm}^2/\text{sec}$  is therefore considered to be in good agreement with the value for sintered compacts. In both diffusion coefficient and activation energy the data for sintered spheroids of both groups are in fair agreement, and the data for the powders are in excellent agreement, with the data for sintered compacts. The most notable exception is sample B3, but as discussed above, the surface area value is suspected to be high. This results in a low value for the derived diffusion coefficient.

All the diffusion data for both sintered spheroids and the powder specimens are compared in Figure 6. On the same figure is shown the line corresponding to the mean for sintered compacts (6). Although at first sight it appears that a closer approximation to the present data could be obtained with a higher activation energy, closer inspection of Figure 6 and Table II shows that those points which lie substantially below the value for sintered compacts at the lower temperatures do so largely because of their low value of  $D_{1400}$  and not as a result of a significantly higher activation energy. We may therefore conclude that, within a factor

of five in diffusion coefficient, the expression

$$D = 7.6 \times 10^{-6} \exp(-70,000/RT) \text{ cm}^2/\text{sec}$$

adequately describes the diffusion kinetics in the post-irradiation emission of xenon-133 from lightly irradiated samples of sintered or powdered uranium dioxide. Any differences between sintered compacts of gram size, sintered spheroids of about 50 microgram size and fine powders are experimentally undetectable.

A series of experiments was performed using sample A1 to investigate the effect of the irradiation time on the observed diffusion parameters. Irradiations were carried out in the range 0.25 to 2 times the standard irradiation dose of  $2.4 \times 10^{17}$  nvt ( $\equiv 2.4 \times 10^{16}$  fissions/cc). The results are plotted in Figure 1. The scatter is high since with the short irradiations the xenon-133 activity evolved was small, and no significant trends are detectable.

With the fused spheroids, the "as-received" material showed abnormally high initial bursts, sufficiently high to confuse the  $f$  vs  $\sqrt{t}$  plots and give rise to erratic results (Figure 3). Values of both  $D_{1400}$  and  $E$  are both lower than the values for sintered material (Table II). After annealing, the value of  $D$  is still low, but the activation energy is substantially increased. Indeed the data for both the "as-received" and annealed material are in good agreement with the corresponding values reported by Stevens et al (7) for single-crystal material prepared by crushing and sieving fused uranium dioxide. It thus appears that the act of fusion, albeit for only a short period in a plasma torch, markedly influences the diffusion behaviour in post-irradiation heating experiments. Furthermore the fact that the plasma-fused material is still polycrystalline, of grain-size about  $15\mu$ , demonstrates that the effect is associated with the process of fusion rather than the monocrystalline form of the powder prepared by crushing bulk-fused material.

In a series of experiments the emission of the volatile fission products from the various samples was followed as a function of time, and the results are presented and discussed in Reference 8.

#### ACKNOWLEDGEMENTS

The authors are indebted to Messrs. C. Wheatley and J. Hedger of A.E.R.E. Harwell and Mr. H. Garrett of A.W.R.E. Aldermaston for the supply of samples, and to Mr. R.H. Brooks for assistance in the laboratory.

#### REFERENCES

1. Booth, A.H. and Rymer, G.T. Determination of the Diffusion Constant of Fission Xenon on  $\text{UO}_2$  Crystals and Sintered Compacts. AECL-CRDC-720.
2. Lindner, von R. and Matzke, HJ. Diffusion radioaktiver Edelgase in Uranoxyden und Uranmonokarbid. Zeit. fur Naturforsch. 14a 1074 (1959).
3. Davies, D. and Long, G. Equipment for the investigation at the emission of Fission Products from irradiated ceramic fuels. AERE - R 4322 (1963).
4. Biddle, P and Long, G. The Characterisation of  $\text{UO}_2$  compacts. AERE - R 3384 (1960).
5. Davies, D and Long, G. Abnormal Kinetics in the release of Inert Gases from Uranium Dioxide. AERE - M 969 (1963).
6. Davies, D. and Long, G. To be published.
7. Stevens, W.H., MacEwan, J.R. and Ross, A.M. The Diffusion behaviour of Fission Xenon in  $\text{UO}_2$ . Proc. 1st Conf. Nuclear Reactor Chemistry, TID-7610 Gatlinburg(1960).
8. Davies, D., Long, G. and Stanaway, W.P. The Emission of Volatile Fission Products from Uranium Dioxide. A.E.R.E. - R 4342 (1963).

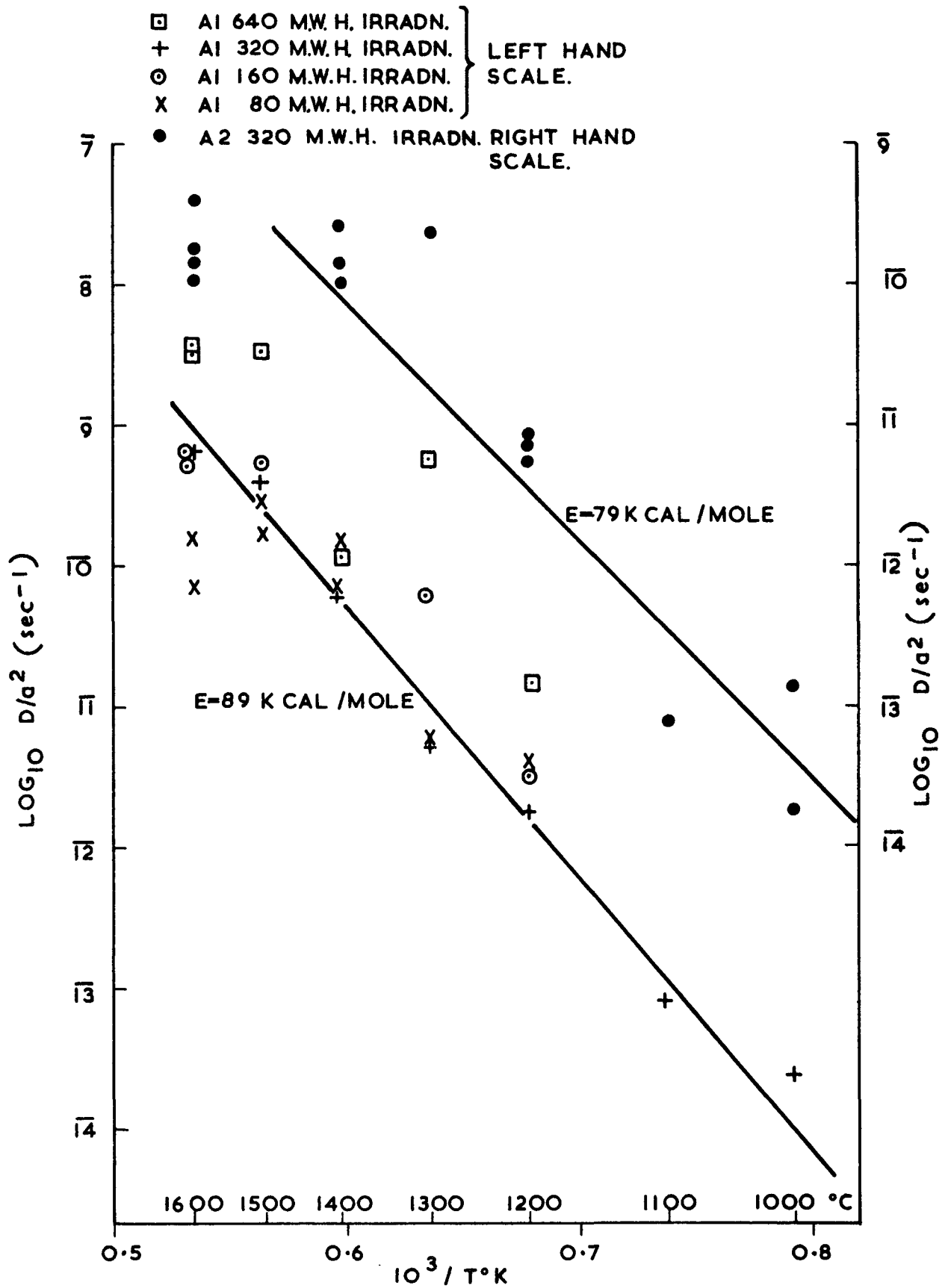
**TABLE I****Physical Properties of UO<sub>2</sub> Spheroids and Powders**

Sample Type	No.	Mean Radius ( $\mu$ )	B.E.T. Area ( $\text{cm}^2/\text{g}$ )	Equiv. Sphere Radius ( $\mu$ )	Roughness Factor
Sintered Spheroid	A1	150	25	114	1.3
Group A	A2	40	103	29	1.5
Sintered Spheroid	B1(a)	>200	-	-	-
Group B	B1(b)	110	88	33	3.3
	B2	150	23	125	1.2
	B3	120	55	52	2.3
Fused Spheroid	F1	60	200	14	4.3
	F2	60	115	25	2.4
Ditto, Annealed	F1/A	60	75	38	1.6
	F2/A	60	77	37	1.6
Powder	P1	-	9,100	0.31	-
	P2	-	1,300	2.2	-

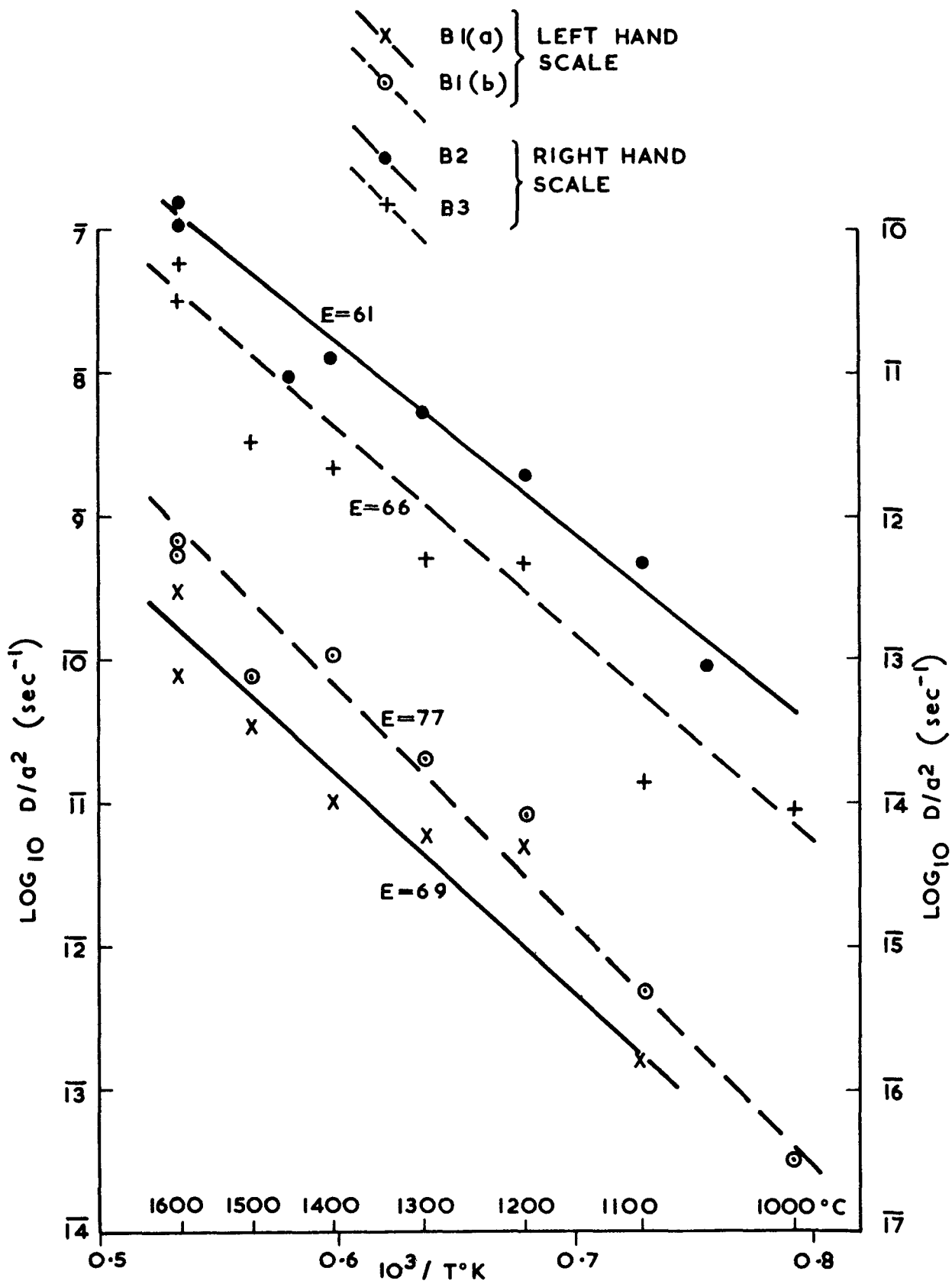
TABLE II

Diffusion Parameters of UO<sub>2</sub> Spheroids and Powders

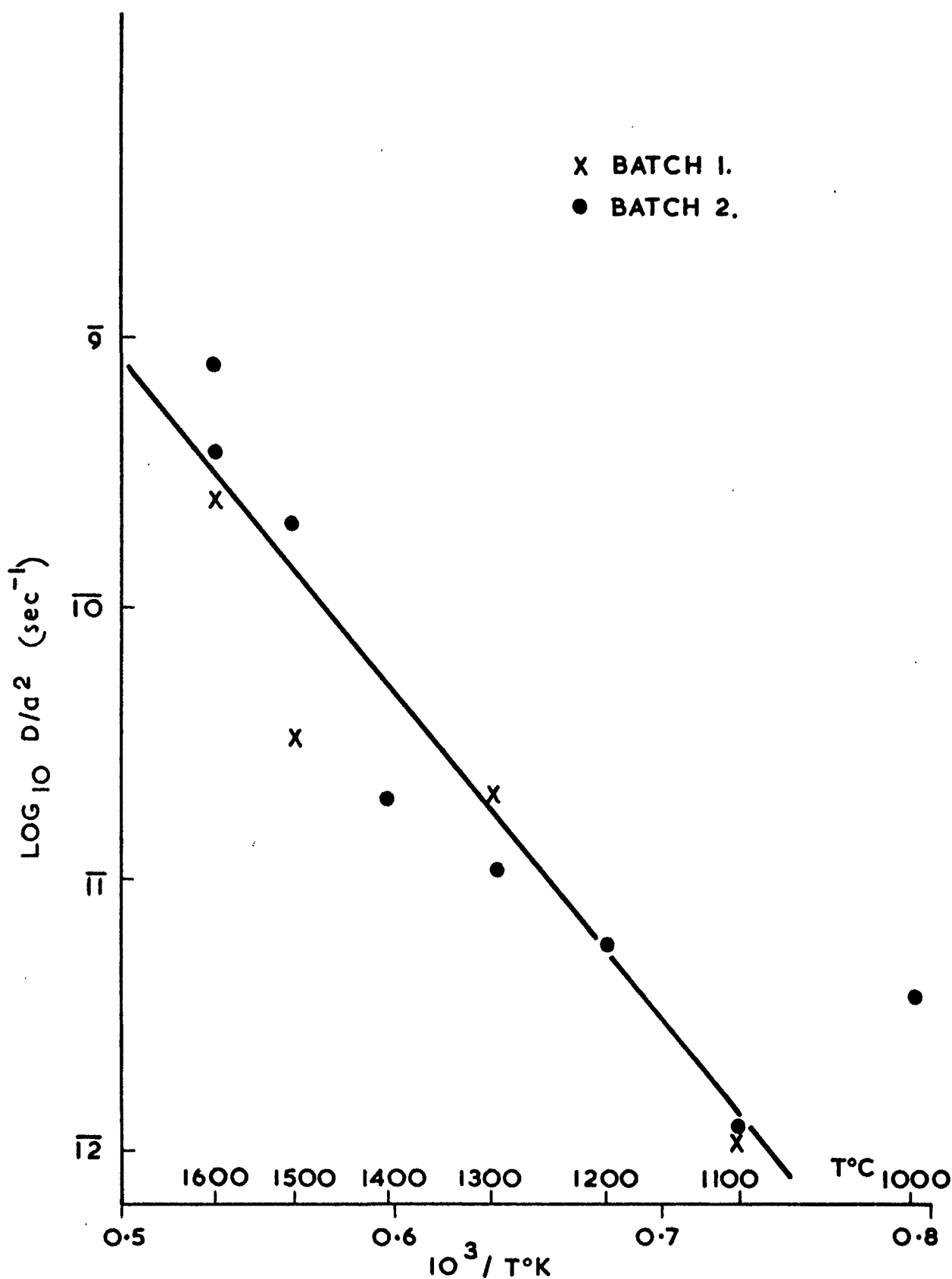
Sample Type	No.	Temp. Range (100°C)	Figure	Mean $D_{1400}^1$ (sec <sup>-1</sup> )	Mean $D_{1400}$ (cm <sup>2</sup> /sec)	Apparent Activation Energy (E) (kcal/mole)	$\left(\frac{D'}{\bar{D}'} \text{ calc.}\right)^{1/2}$ at 1400°C
Sintered Spheroid Group A	A1	10-16	1	$5.7 \times 10^{-11}$	$7.2 \times 10^{-15}$	89	1.6
	A2	"	1	$9.0 \times 10^{-11}$	$8.0 \times 10^{-16}$	79	0.6
Sintered Spheroid Group B	B1(a)	11-16	2	$1.6 \times 10^{-11}$	-	69	1.1
	B1(b)	10-16	2	$7.4 \times 10^{-11}$	$8.0 \times 10^{-16}$	77	1.4
	B2	"	2	$1.7 \times 10^{-11}$	$2.5 \times 10^{-15}$	61	0.9
	B3	"	2	$4.3 \times 10^{-12}$	$1.0 \times 10^{-16}$	66	0.4
Fused Spheroid	F1	11-16	3	$5.0 \times 10^{-11}$	$1.0 \times 10^{-16}$	-56	0.7
	F2	"	3	$5.0 \times 10^{-11}$	$3.0 \times 10^{-16}$	-56	0.7
Ditto, Annealed	F1/A	"	4	$2.8 \times 10^{-11}$	$4.0 \times 10^{-16}$	100	0.5
	F2/A	"	4	$2.8 \times 10^{-11}$	$4.0 \times 10^{-16}$	100	0.5
Powder	P1	8-11	5	$*8.0 \times 10^{-7}$	$*8.0 \times 10^{-16}$	72	-
	P2	10-14	5	$6.3 \times 10^{-8}$	$3.1 \times 10^{-15}$	68	-
*Extrapolated Values							



AERE. R.4347. FIG.1.  
 PLOTS OF LOG<sub>10</sub> D/a<sup>2</sup> (sec<sup>-1</sup>) VERSUS  $\frac{1}{T^{\circ}K}$  FOR SINTERED  
 SPHEROIDS OF GROUP A.

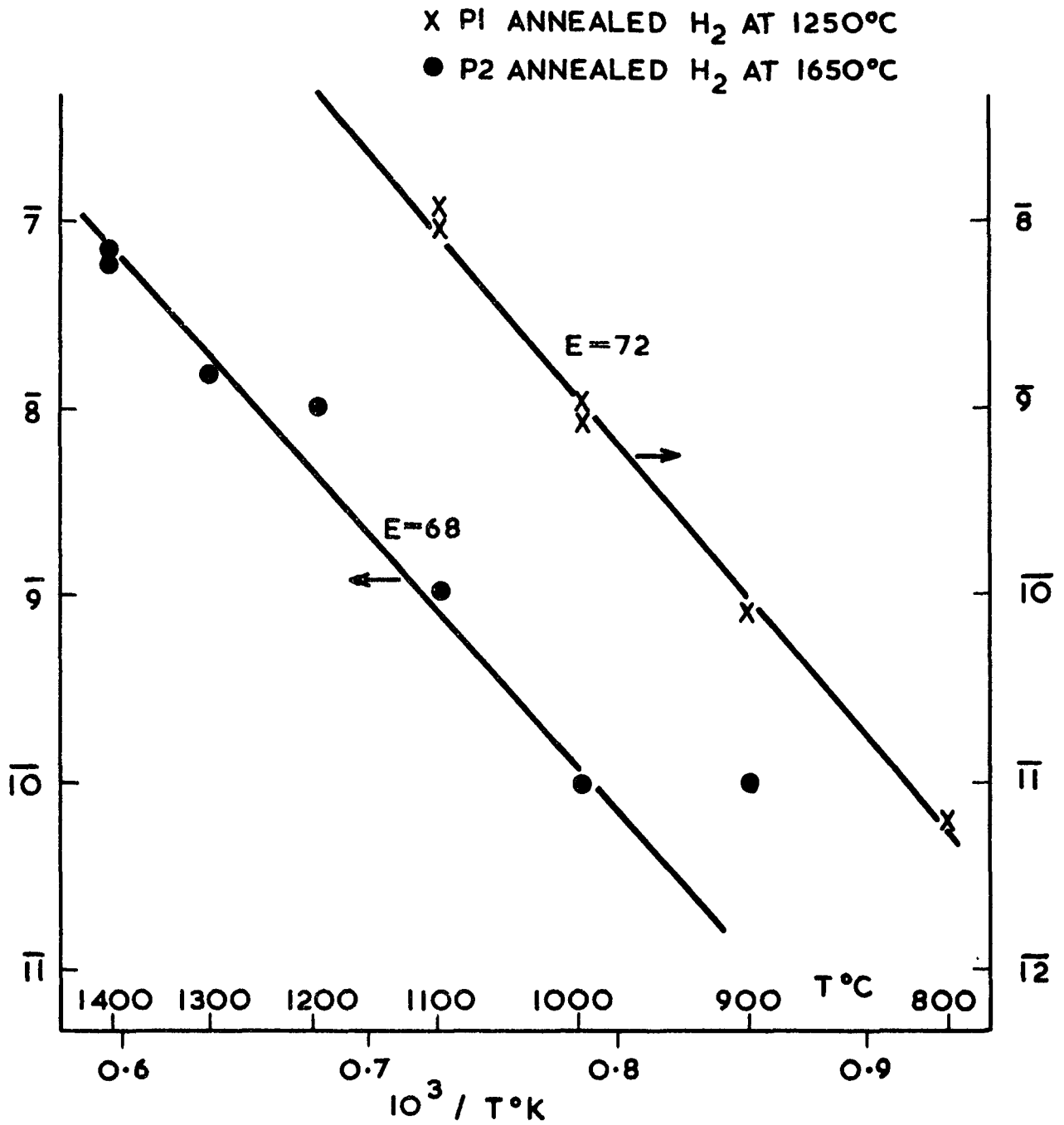


AERE. R.4347. FIG. 2.  
 PLOTS OF LOG<sub>10</sub> D/a<sup>2</sup> (sec<sup>-1</sup>) VERSUS  $\frac{1}{T^{\circ}\text{K}}$  FOR SPHEROIDS  
 OF GROUP B.



AERE. R.4347. FIG. 3.  
 PLOT OF  $\log_{10} D/a^2$  (sec<sup>-1</sup>) VERSUS  $\frac{1}{T^{\circ}K}$  FOR PLASMA-FUSED SPHEROIDS (AS RECEIVED)





AERE. R.4347. FIG 5.

PLOTS OF  $\log_{10} D/a^2$  (sec<sup>-1</sup>) VERSUS  $\frac{1}{T^\circ K}$   
 FOR SAMPLES OF URANIUM DIOXIDE POWDER.

